RECENT ADVANCES ON LIQUID CRYSTAL BASED RECONFIGURABLE ANTENNA ARRAYS

Saygin Bildik[1], Onur H. Karabey[1], Sabine Dieter[2], Carsten Fritzsch[1], Alexander Gaebler[1], Rolf Jakoby[1], and Wolfgang Menzel[2]

[1]*Institute for Microwave Engineering and Photonics, Technische Universitaet Darmstadt, Merckstr. 25, 64283 Darmstadt, Germany*
bildik@imp.tu-darmstadt.de
[2]*Institute of Microwave Techniques, University of Ulm, Albert-Einstein-Allee 41, 89081 Ulm, Germany*

ABSTRACT

A reflectarray and a phased array antenna, which are based on the liquid crystal technology, are designed and realized. The reflectarray is composed of 16×16 antenna elements. The elements are based on coupled microstrip patches. The proposed coupled microstrip structure exhibits a tunable phase range of more than 360° at 77 GHz and has the advantage of being broadband. The phased array, which is only 1.5 mm-thick, consists of 2×2 elements. 2-D beam steering capability of the phased array shows that the proposed antenna advances state of the art for the liquid crystal based phased arrays, which are limited to scan only in one dimension so far. Beam steering capabilities of the antenna arrays are presented by successfully steering the main beams to various angles.

Key words: Microstrip antenna arrays; reflectarrays; liquid crystals; beam steering; patch antennas; microwave antennas; millimeter wave technology.

1. INTRODUCTION

Liquid crystals (LCs) are well-known as one of the optical components of LCD screens, where their anisotropy plays an essential role for controlling the polarization of light. Besides the optical region, the anisotropy of LCs can be used in the microwave spectrum beginning from 10 GHz [1–3]. They consist of elongated rod-like molecules and exhibit different electrical characteristics depending on how an RF-field is incident on the molecules [4]. A desired permittivity can be achieved by controlling the molecule orientation with respect to the RF-field. Therefore, LCs can be used as tunable substrates. The molecules tend to align along either electric or magnetic external fields, which can be used to control the orientation of the entire LC bulk. Additionally, they can be oriented by surface anchoring, which is generally preferred for the pre-alignment of the LC bulk [4].

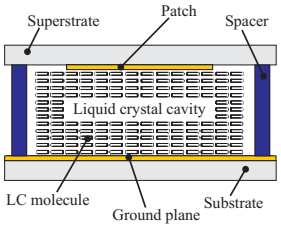

Figure 1. Cross-section of an LC filled antenna element.

Microwave antennas, which benefit from the continuous tunability of LCs, have been designed with different capabilities for different purposes. Reconfigurable reflectarrays [5–7] and phased arrays [8, 9] for continuous beam steering, frequency agile antennas [10, 11] for changing the operating frequency and polarization agile antennas [12, 13] for polarization reconfigurability have been successfully realized so far as LC based antennnas. In this paper, a reconfigurable reflectarray antenna with extended tunable phase range [14] and a two-dimensional (2-D) electronically-steered phased array antenna [15] are presented. The reflectarray is composed of coupled microstrip structures (three fingerlike patches) to extend the phase angle range of the antenna elements. The phased array, which operates at 17.5 GHz, includes LC based variable delay lines in inverted microstrip line (IMSL) topology [16].

2. RECONFIGURABLE REFLECTARRAY WITH EXTENDED TUNABLE PHASE RANGE

2.1. Antenna Element

The IMSL topology depicted in Fig. 1 is used to build a tunable microstrip reflectarray element. The antenna element comprises a substrate, a ground plane, a liquid crystal cavity, a microstrip patch and a superstrate. The upper part of the substrate is completely metallized to form the ground plane, and the patch is printed beneath the super-

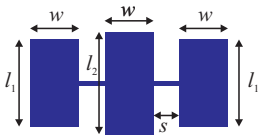

Figure 2. Drawing of the designed coupled patches.

Table 1. Dimensions of the designed patch.

l_1 [mm]	l_2 [mm]	w [mm]	s [mm]
0.975	1.025	0.5	0.2

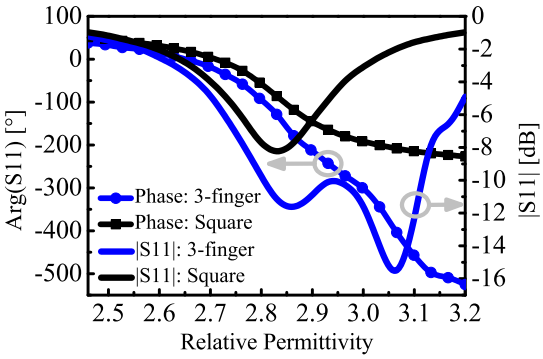

Figure 3. Simulation results of three-fingerlike patch and square patch elements at 77 GHz.

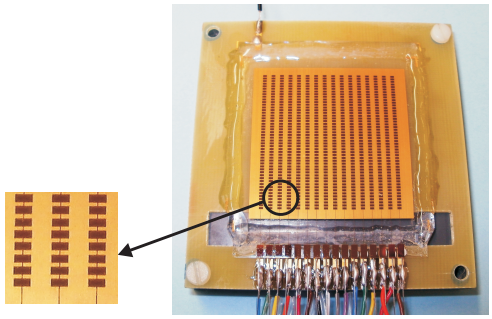

(a)

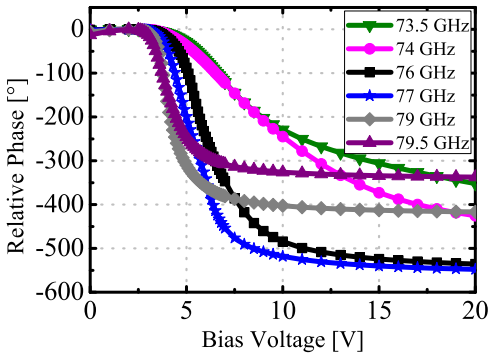

(b)

Figure 4. Photograph of the realized reflectarray (a) and measured relative phase shift (b).

strate. The liquid crystal cavity is formed between the superstrate and the ground plane with the aid of spacers.

Various shapes of microstrip patches have been examined in [17] by using a lumped-element model for the antenna elements. Furthermore, to extend the phase angle range of the antenna elements and to reduce the slope of the phase angles, coupled structures consisting of patches printed on a non-tunable substrate are presented in [18]. Within the aforementioned coupled structures, a three-fingerlike patch design (see Fig. 2) is the most proper one for the LC technology in terms of biasing. The thin line connecting three patches to each other can be used as a part of a bias line.

The antenna element (unit cell) has been designed for the LC mixture LC-C1 given in [14] and dimensions of the proposed patch are presented in Tab. 1. A unit cell length of 2.14 mm ($0.55\lambda_0$ at 77 GHz) and an LC cavity thickness of 50 µm are set for the antenna elements. As illustrated in Fig. 3, the coupled patch element has a 563° tunable phase range ($\Delta\varphi$) while a square-shaped reference patch element [14] has only 277° at 77 GHz. A comparison can also be done in terms of another quantity named figure-of-merit (FoM) that is defined as $\frac{\Delta\varphi}{\text{Maximum loss}}$. Although the three-fingerlike patch cell has higher losses, it has a FoM of 36.4 °/dB, which is more than the FoM of square one (33.8 °/dB), due to the wider phase range.

In comparison to the square patches, thus gaps in the phase adjustment can be avoided. Furthermore, since the coupled structure produces more than 360° of phase shift with the voltage range of 0 V to 20 V, not only the phases but also the amplitude variations of the elements can be taken into account within pattern synthesis. This can be performed by selecting necessary phase values with lower losses.

2.2. Antenna Realization and Characterization

The fabricated antenna array consists of 16×16 patch elements with an element spacing of $0.55\lambda_0$. In order to tune the LC molecules, each sixteen patches, which are in the same row, are connected by the same bias lines. Therefore, the elements which belong to the same row yield the same phase, and hence the main beam of the reflectarray can be steered in one plane. For that reason, a feed with a line source characteristics is required to illuminate the antenna. The bias lines are placed perpendicular to the resonant lengths l_1 and l_2 of the patch elements (see Fig. 4a), and the width of the lines is set to 50 µm for the proposed topology to prevent interference with the RF-field.

300 µm-thick fused silica plates are used as substrates to carry the patch and ground plane electrodes (see Fig. 1). The loss tangent of the fused silica is below 0.0015 up to 90 GHz while the relative permittivity is 3.8 [19]. In order to form the LC cavity, commercially available micro pearls with a diameter of 50 µm are used as cavity

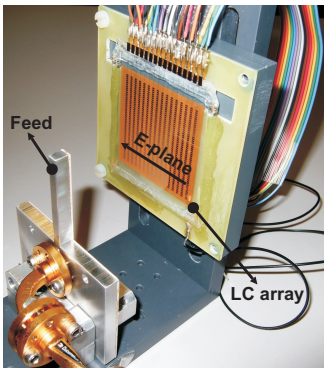

(a)

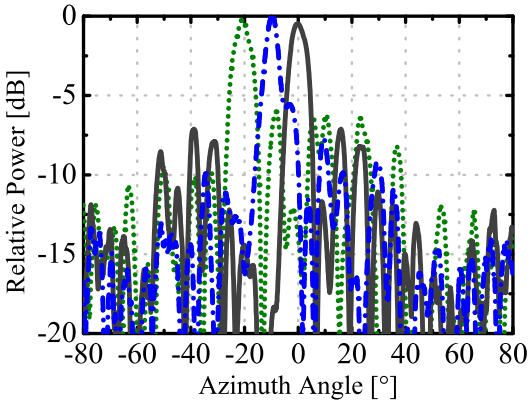

(b)

Figure 5. Photograph of the reflectarray setup (a) and measured far-field patterns at 77 GHz (b).

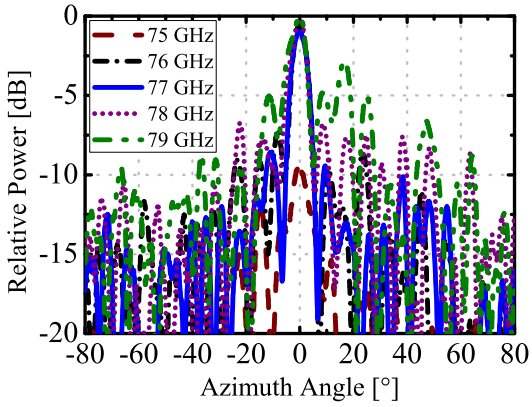

(a)

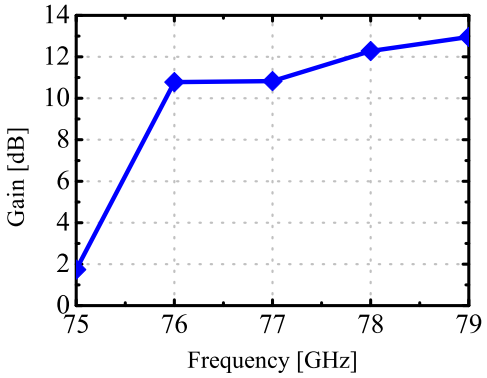

(b)

Figure 6. Measured far-field patterns at different frequencies (a) and measured antenna gain over frequency (b).

spacers. Micro pearls are mixed with glue and inserted between the two fused silica plates by avoiding the active region of the array to form a 50 µm-thick cavity.

After filling the reflectarray with the LC mixture (LC-C1), the antenna shown in Fig. 4a (reflector part) is characterized by a quasi-optical lens setup [20]. Measurements are carried out by applying the same bias voltages (0 V to 20 V) to each antenna element row. Fig. 4b depicts the tuning capability of the realized antenna in terms of $\Delta\varphi$ measured as 546° at 77 GHz. Antenna elements based on the coupled microstrip patches exhibit a broadband behavior due to having two different resonant frequencies. Measurement results show that the realized reflectarray is able to generate more than 300° relative phase shift in the frequency range of 73.5 GHz to 79.5 GHz when the bias voltage is changed from 0 V to 15 V.

2.3. Far-field Measurements

A feed based on a slotted substrate integrated waveguide technology is used to illuminate the reflectarray [14]. A photograph of the reflectarray setup is shown in Fig. 5a including the feed and the LC based reflector. Owing to the one-dimensional reconfigurability, beam-forming is performed by the reflectarray in the E-plane. In the H-plane, the beam characteristic is obtained by the feed. Fig. 5b presents the measured far-field diagrams of the reflectarray antenna at 77 GHz for three different main beam directions 0°, −10° and −20°. Amplitude change due to the beam steering is negligible and sidelobe levels of −6.7 dB, −7.7 dB and −5.9 dB are obtained for the beam directions of 0°, −10° and −20°, respectively. The steering ability of the antenna is not only limited to the above mentioned angles. The main beam can be also steered to different angles continuously because of capabilities of the LC technology. Bias voltages have been obtained by using the near-field characterization results [21] that allow to characterize antenna elements individually instead of the overall array characterization performed with the quasi-optical measurements.

As can be seen in Fig. 6a, the realized antenna is viable in the frequency range of 76 GHz to 78 GHz without changing the bias voltage configuration. It should be noted that the applied voltage configuration has been obtained for 77 GHz. Significant distortions in the antenna pattern are observed at 75 GHz and at 79 GHz. This may result from the differential spatial phase delay, which can be mitigated by increasing the focal-length-to-diameter ratio

(f/D) with the aim of reducing the differences between paths from the feed to the reflectarray elements. Alternatively, different bias voltage configurations can be used for different frequency intervals.

The measured gain of the reflectarray antenna is 11 dB at 77 GHz (see Fig. 6b) and the steep reduction in the antenna gain at 75 GHz is due to the matching of the feed.

3. ELECTRONICALLY-STEERED PHASED ARRAY ANTENNA

3.1. Description of the Phased Array Antenna

The proposed phased array antenna consists of identical unit elements, comprising a radiating element, a voltage tunable delay line, a bias line and a dc blocking structure. A block diagram of the unit element is given in Fig. 7. Two feeding networks are required in order to deliver both RF and bias signals individually to all unit elements. It should be mentioned that the proposed antenna is not a modular-based antenna, which refers that several unit elements are built separately and then combined to form the array. Indeed, the components of the array, which are implemented on the same substrate, are fabricated simultaneously. Later on different layers are combined to form the final structure. However, the unit element is explained herein to give a clear understanding of the different layers, and the operation principle.

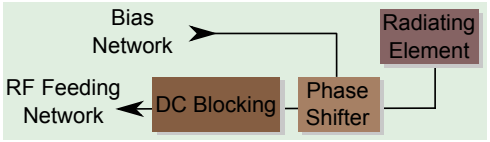

Figure 7. Block diagram of the unit element of the phased array antenna.

The unit element is fabricated by using three dielectric layers, namely front, LC and back dielectric layers. Schematics of the unit element are depicted in Fig. 8.

A microstrip patch antenna is mounted on the top side of the front dielectric substrate. The ground electrode of the patch antenna is mounted on the bottom side of the same substrate. The ground electrode includes a slot overlying the patch (Fig. 8c), which forms an aperture coupling between the patch antenna and the variable delay line. The delay line is implemented in IMSL topology. Owing to the IMSL topology, the delay line can be bended and provides high performance [22]. The signal electrode of the IMSL is mounted on the top side of the back substrate. The LC material is encapsulated between the two substrates. The tunable LC material forms the dielectric of the IMSL and has a thickness of 100 µm.

A 700 µm-thick glass, namely Borofloat®, from Schott AG is utilized for the front and back substrates. Its

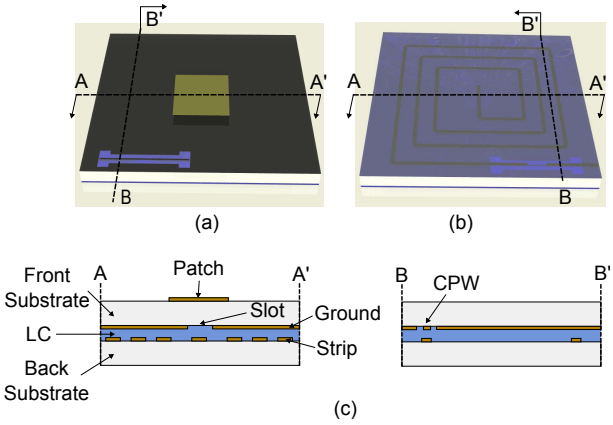

Figure 8. Schematics of the unit element. (a) Top-perspective, (b) bottom-perspective and (c) cross sectional views.

electrical properties are specified as $\varepsilon_r = 4.6$ and $\tan\delta = 0.0037$ at 25 °C and at 1 MHz by the manufacturer. The relative permittivity of the LC sample can be tuned between $\varepsilon_r = 2.4$ and $\varepsilon_r = 3.2$ by applying a bias voltage across the signal and ground electrodes of the IMSL. The maximum dielectric loss tangent $\tan\delta$ of this material is less than 0.006 for all tuning states.

In operation of a receiving antenna, the received RF signal is first coupled from the patch antenna to the delay line. While propagating along the delay line, the phase of the signal can be tuned by controlling the relative permittivitiy of the LC layer. At the end of delay line, the RF signal is electromagnetically coupled to a coplanar waveguide (CPW), which is located on the ground electrode. The RF signal propagates along the short CPW line, and then it is coupled to the unit element input port, which is placed on the top side of the back substrate. In this way, a contactless RF interconnection is accomplished as a DC blocking structure between the IMSL and the unit element input port.

Before a complete antenna is fabricated, a meandered variable delay line is fabricated and tested. The details can be found in [15]. During the measurements, a DC-biasing voltage, which is in the range of 0 V to 40 V, is applied in a step of 1 V to orient the LC molecules. The insertion losses are measured less than 4 dB when the return losses are about 15 dB for the all tuning states. According to these results, the delay line provides a maximum differential phase shift of 300° at the operating frequency of 17.5 GHz.

3.2. Antenna Protoype and Measurement Results

An antenna demonstrator with 2×2 unit elements is built as a proof of concept. Its photographs are shown in Fig. 9. An SMA and a four-pin DC connectors are implemented for the RF signal and bias voltage, respectively. As it is seen from the figure, the planar antenna has an overall

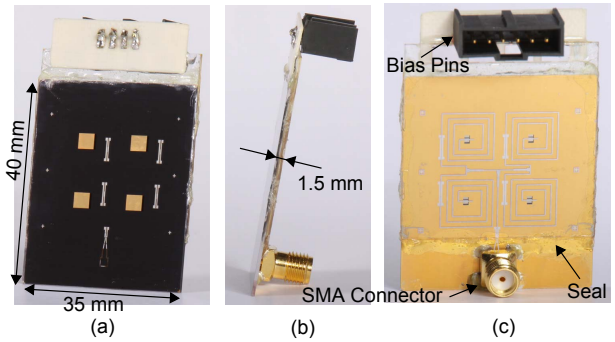

Figure 9. Photographs of the 2×2 array antenna. (a) Top, (b) side and (c) back views.

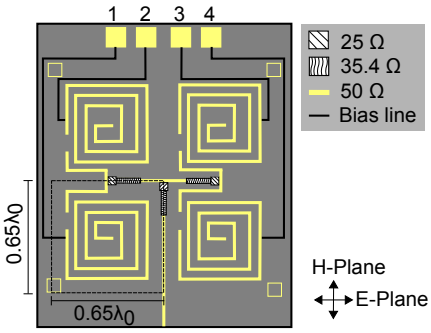

Figure 10. A layout of the 2×2 array antenna. The layout shows the components mounted on the top side of the back dielectric layer. These components are RF-feeding network, variable delay line, biasing network and four biasing pads.

thickness of only 1.5 mm. Another antenna without the bias lines is fabricated as well in order to use as a reference antenna for quantizing the effects of the chromium (Cr) bias lines on the antenna characteristics.

Fig. 10 shows the layout of the components, which are implemented on the top side of the back substrate (see Fig. 8). As previously mentioned, four IMSLs are fabricated simultaneously on this layer. Additionally, the IMSLs are combined by means of a RF-feeding network, which delivers the RF signal equally in magnitude and in phase. Furthermore, a biasing network consisting of bias pads and bias lines are located on the same layer.

The bias lines are fabricated by using a low electrically conductive material that is a Cr material to neglect their impact on the RF circuitry. They have a thickness of 5 nm, which results in a sheet resistance of 25.3 Ω/sq. The line width is set to be 10 µm to increase the bias line resistance. The corresponding DC resistances between the bias pads and the delay line are measured around 160 kΩ to 900 kΩ.

The 10 dB fractional bandwidths of the reference antenna and the simulations are about 10 %. The reference antenna has a return loss of less than 20 dB from 17.5 GHz to 18.3 GHz. The reflection coefficients of the steerable

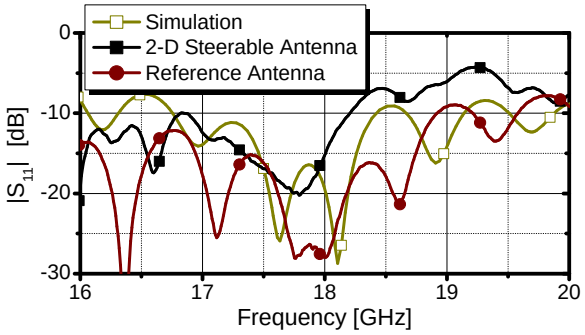

Figure 11. Magnitude of the reflection coefficients of the antenna arrays. 2-D steerable antenna includes the bias lines and the reference antenna is fabricated without the bias lines.

Table 2. Applied voltages for the beam steering

(V)				Beam Steering in	Beam Steering in
V_1	V_2	V_3	V_4	E-Plane	H-Plane
0	0	0	0	0°	0°
13	0	0	13	30°	0°
0	11	11	0	-15°	0°
10	10	0	0	0°	20°
0	0	12	12	0°	-18°

antenna are higher compared to those of the reference antenna. Specifically, its 10 dB fractional bandwidth is about 8 % that is centered at around 17.5 GHz. Empirical studies show that as the conductivity of the bias line increases, the return loss of the antenna array increases as well.

The radiation patterns of the steerable antenna are measured inside an anechoic chamber. During the measurements, the radiated power from a transmitter antenna is received by the prototype and it is measured by using a power meter. The prototypes are placed on a turn table by which the radiation characteristics are measured separately for E- and H-planes, to present 2-D beam steering capability.

In Fig. 12 and in Fig. 13, the far field power pattern measurements are given for the E- and H-planes, respectively, at 17.5 GHz. The antenna main beam can be steered to any desired direction, since the phase of the LC based variable delay line can be tuned continuously. However, the beam steering is presented only for three cases herein and further details are given in [15]. In Tab. 2, the voltages that are applied to the biasing pads are given in detail.

The measured and estimated gains in the E- and H-plane are plotted in Fig. 14 for different main beam directions Θ_m. The measured gains are 0.5 dB to 1.5 dB less than the estimated values because of two expected reasons. First, the Cr bias lines increase the delay line inser-

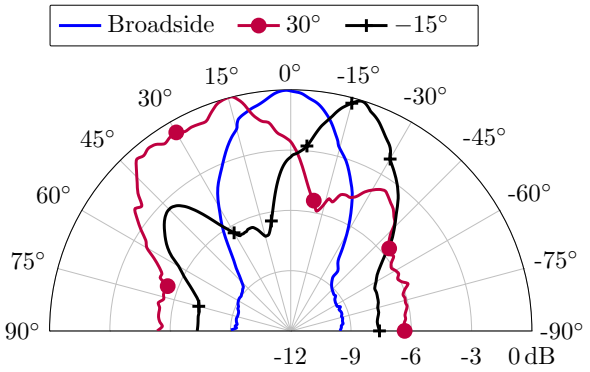

Figure 12. Antenna far-field power pattern measurement results for the E-plane.

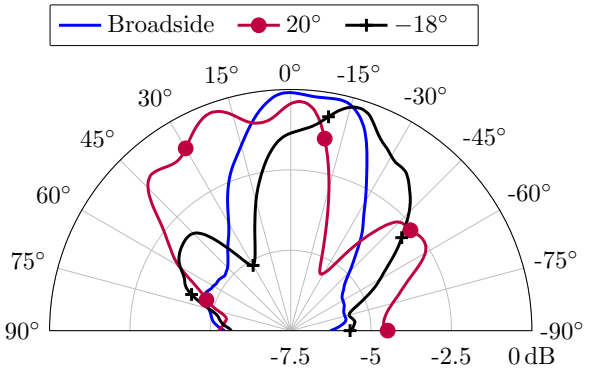

Figure 13. Antenna far-field power pattern measurement results for the H-plane.

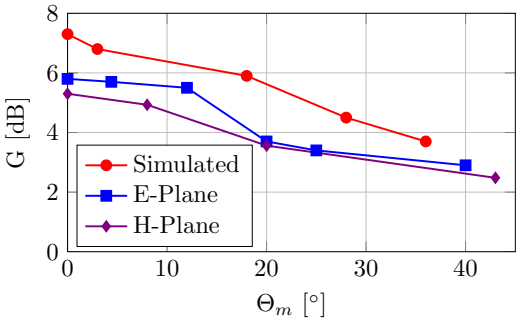

Figure 14. Estimated and measured antenna gains over main beam direction Θ_m.

tion loss, which reduces the transmission, and therefore the antenna gain. Second, the connections and adaptors used in the measurement setup add additional losses. Due to the fabrication tolerances, the measured gains in the E- and H-plane differ less than 1 dB.

4. CONCLUSION

A reconfigurable reflectarray antenna with extended tunable phase range and a 2-D electronically-steered phased array antenna are presented as prototypes of liquid crystal based antenna arrays. The realized reflectarray is composed of 16×16 elements in which coupled microstrip patches are used to extend the phase angle range of the antenna elements and to achieve more gradual phase curves. Furthermore, since the proposed coupled structure is a wideband antenna element, it gives the opportunity to improve the bandwidths of reflectarrays. The one-dimensional beam steering capability of the reflectarray is demonstrated by successfully steering the main beam to 0°, −10° and −20°. This antenna may be used in radar, wireless communication and remote sensing applications.

The realized phased array consists of a 2×2 microstrip patch elements, continuously variable delay lines with a novel geometry, an RF-feeding and a bias network. Such an antenna is utilized to provide various services such as wireless internet, multimedia, communication, and broadcasting services from terrestrial systems and satellites to a mobile terminal, e.g. automobiles and airplanes.

The fabrication technology of proposed antennas combines LC display and printed circuit board technologies. Therefore, the arrays with many elements can be fabricated with a simple and low-cost automated manufacturing techniques. The arrays can be produced larger by increasing the number of elements. Alternatively, several arrays can be integrated with each other to build a larger array, e.g. 4 pieces of 16×16 reflectarray can be combined to obtain a 32×32 reflectarray.

ACKNOWLEDGMENT

Reflectarray work has been supported by the DFG-Project ”Rekonfigurierbare Millimeterwellen-Antennen mit steuerbaren hoch-anisotropen Fluessigkristallen”. The authors would like to thank Merck KGaA for providing the employed liquid crystals and for the financial support of the phased array antenna project. Special thanks are reserved for CST GmbH, which provides CST Microwave Studio.

REFERENCES

1. S. Mueller, A. Penirschke, C. Damm, P. Scheele, M. Wittek, C. Weil, and R. Jakoby, “Broad-band microwave characterization of liquid crystals using a temperature-controlled coaxial transmission line,” *IEEE Transactions on Microwave Theory and Techniques*, vol. 53, no. 6, pp. 1937–1945, Jun. 2005.

2. S. Bulja, D. Mirshekar-Syahkal, R. James, S. Day, and F. Fernadez, “Measurement of Dielectric Properties of Nematic Liquid Crystals at Millimeter Wavelength,” *IEEE Transactions on Microwave Theory and Techniques*, vol. 58, no. 12, pp. 3493–3501, Dec. 2010.

3. S. Mueller, F. Goelden, P. Scheele, M. Wittek, C. Hock, and R. Jakoby, "Passive Phase Shifter for W-Band Applications using Liquid Crystals," in *Proc. 36th European Microwave Conference*, Sep. 10–15, 2006, pp. 306–309.

4. D.-K. Yang and S.-T. Wu, *Fundamentals of Liquid Crystal Devices*. John Wiley & Sons, Ltd, 2006.

5. R. Marin, A. Mossinger, J. Freese, A. Manabe, and R. Jakoby, "Realization of 35 GHz Steerable Reflectarray using Highly Anisotropic Liquid Crystal," in *Proc. IEEE Antennas and Propagation Society International Symposium 2006*, 2006, pp. 4307–4310.

6. A. Moessinger, R. Marin, S. Mueller, J. Freese, and R. Jakoby, "Electronically reconfigurable reflectarrays with nematic liquid crystals," *Electronics Letters*, vol. 42, no. 16, pp. 899–900, Aug. 2006.

7. W. Hu, M. Ismail, R. Cahill, J. Encinar, V. Fusco, H. Gamble, D. Linton, R. Dickie, N. Grant, and S. Rea, "Liquid-crystal-based reflectarray antenna with electronically switchable monopulse patterns," *Electronics Letters*, vol. 43, no. 14, 2007.

8. G.-A. Chakam, W. Vogel, H. Yilmaz, M. Berroth, and W. Freude, "Microstrip phased array patch antenna based on a liquid crystal phase shifter for optically generated RF-signals," in *Microwave Photonics, 2002. International Topical Meeting on*, nov. 2002, pp. 265 – 268.

9. B. Sanadgol, S. Holzwarth, and J. Kassner, "30 GHz liquid crystal phased array," in *Antennas Propagation Conference, 2009. LAPC 2009. Loughborough*, nov. 2009, pp. 589 –592.

10. L. Liu and R. Langley, "Liquid crystal tunable microstrip patch antenna," *Electronics Letters*, vol. 44, no. 20, pp. 1179 –1180, 25 2008.

11. C. Fritzsch, S. Bildik, and R. Jakoby, "Ka-Band Frequency Tunable Patch Antenna," in *2012 IEEE International Symposium on Antennas and Propagation*, 2012, accepted paper.

12. O. Karabey, S. Bildik, S. Strunck, A. Gaebler, and R. Jakoby, "Continuously polarisation reconfigurable antenna element by using liquid crystal based tunable coupled line," *Electronics Letters*, vol. 48, no. 3, pp. 141 –143, 2 2012.

13. O. Karabey, S. Bildik, S. Bausch, S. Strunck, A. Gaebler, and R. Jakoby, "Continuously Polarization Agile Antenna by Using Liquid Crystal Based Tunable Variable Delay Lines," *Antennas and Propagation, IEEE Transactions on*, vol. PP, no. 99, p. 1, 2012.

14. S. Bildik, S. Dieter, C. Fritzsch, M. Frei, C. Fischer, W. Menzel, and R. Jakoby, "Reconfigurable liquid crystal reflectarray with extended tunable phase range," in *Proc. 41st European Microwave Conf. (EuMC)*, Oct. 2011, pp. 1292–1295.

15. O. Karabey, A. Gaebler, S. Strunck, and R. Jakoby, "A 2-D Electronically Steered Phased-Array Antenna With 2×2 Elements in LC Display Technology," *Microwave Theory and Techniques, IEEE Transactions on*, vol. 60, no. 5, pp. 1297 –1306, may 2012.

16. T. Kuki, H. Fujikake, and T. Nomoto, "Microwave variable delay line using dual-frequency switching-mode liquid crystal," *IEEE Transactions on Microwave Theory and Techniques*, vol. 50, no. 11, pp. 2604–2609, 2002.

17. M. Bozzi, S. Germani, and L. Perregrini, "A figure of merit for losses in printed reflectarray elements," *IEEE Antennas and Wireless Propagation Letters*, vol. 3, no. 1, pp. 257–260, 2004.

18. S. Dieter, C. Fischer, and W. Menzel, "Single-layer unit cells with optimized phase angle behavior," in *Antennas and Propagation, 2009. EuCAP 2009. 3rd European Conference on*, Mar. 23-27 2009, pp. 1149–1153.

19. D. Liu, *Advanced Millimeter-Wave Technologies: Antennas, Packaging and Circuits*. John Wiley & Sons, Ltd, 2009, ch. Antenna Design for 60 GHz Packaging Applications, pp. 295–351.

20. A. Moessinger, S. Dieter, W. Menzel, S. Mueller, and R. Jakoby, "Realization and characterization of a 77 GHz reconfigurable liquid crystal reflectarray," in *Antenna Technology and Applied Electromagnetics and the Canadian Radio Science Meeting, 2009. ANTEM/URSI 2009. 13th International Symposium on*, Feb. 15-18 2009, pp. 1–4.

21. S. Dieter, A. Moessinger, S. Mueller, W. Menzel, and R. Jakoby, "Characterization of Reconfigurable LC-Reflectarrays Using Near-Field Measurements," in *German Microwave Conference, 2009*, Mar. 16-18 2009, pp. 1–4.

22. S. Muller, P. Scheele, C. Weil, M. Wittek, C. Hock, and R. Jakoby, "Tunable passive phase shifter for microwave applications using highly anisotropic liquid crystals," in *Proc. IEEE MTT-S Int. Microwave Symp. Digest*, vol. 2, 2004, pp. 1153–1156.